Constraining dense matter properties with INDRA-FAZIA at GANIL

Caterina Ciampi

GANIL

for the INDRA-FAZIA collaboration

GDR RESANET Plenary meeting

Strasbourg, France
November 3rd - 7th, 2025

Systems of neutrons and protons can be found:

Nuclear matter
Where can we find systems of neutrons and protons?

Systems of neutrons and protons can be found:

- At the **microscopic** level in **nuclei** (density around saturation ρ_0)
  laboratory experiments → collect data on nuclear structure and dynamics

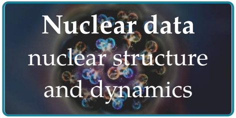

Nuclear matter

Where can we find systems of neutrons and protons?

Systems of neutrons and protons can be found:

- At the **microscopic** level in **nuclei** (density around saturation ρ_0)
  laboratory experiments → collect data on nuclear structure and dynamics
- At the **macroscopic** level in **neutron stars** (density several times ρ_0)
  multimessenger astronomy → wealth of information on neutron star properties

Nuclear data
nuclear structure
and dynamics

Astrophysical data
static and dynamical
properties of NS

Systems of neutrons and protons can be found:

- At the **microscopic** level in **nuclei** (density around saturation ρ_0)
  laboratory experiments → collect data on nuclear structure and dynamics
- At the **macroscopic** level in **neutron stars** (density several times ρ_0)
  multimessenger astronomy → wealth of information on neutron star properties

Nuclear data
nuclear structure
and dynamics

Astrophysical data
static and dynamical
properties of NS

Nuclear matter behavior

Systems of neutrons and protons can be found:

- At the **microscopic** level in **nuclei** (density around saturation ρ_0)
  laboratory experiments $\longrightarrow$ collect data on nuclear structure and dynamics
- At the **macroscopic** level in **neutron stars** (density several times ρ_0)
  multimessenger astronomy $\longrightarrow$ wealth of information on neutron star properties

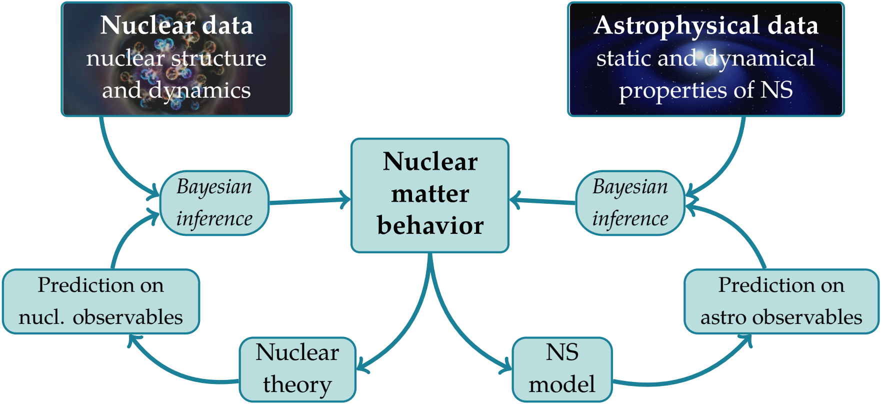

Systems of neutrons and protons can be found:

- At the **microscopic** level in **nuclei** (density around saturation ρ_0)
  laboratory experiments → collect data on nuclear structure and dynamics
- At the **macroscopic** level in **neutron stars** (density several times ρ_0)
  multimessenger astronomy → wealth of information on neutron star properties

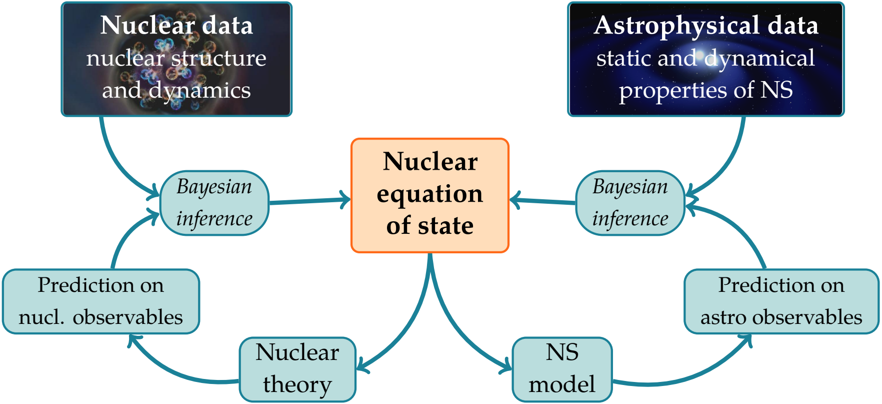

Nuclear Equation of State (nEoS): Thermodynamic description of nuclear matter.
→ energy per nucleon of a uniform system of nucleons, expressed as a function of:

nuclear density: $\rho = \rho_n + \rho_p$

isospin asymmetry: $\delta = \frac{\rho_n - \rho_p}{\rho_n + \rho_p} = \frac{N-Z}{A}$

Nuclear Equation of State (nEoS): Thermodynamic description of nuclear matter.
→ energy per nucleon of a uniform system of nucleons, expressed as a function of:

nuclear density: $\rho = \rho_n + \rho_p$

isospin asymmetry: $\delta = \frac{\rho_n - \rho_p}{\rho_n + \rho_p} = \frac{N-Z}{A}$

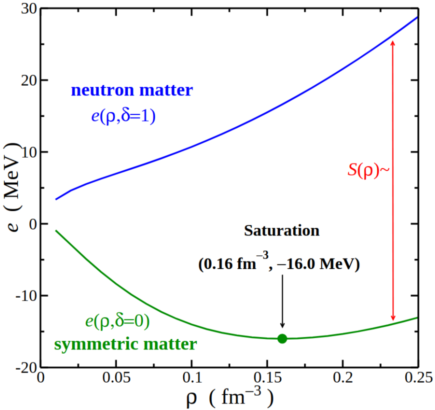

$$e(\rho,\delta) = e(\rho,\delta=0) + S(\rho)\delta^2 + \ldots$$

Nuclear Equation of State (nEoS): Thermodynamic description of nuclear matter.
→ energy per nucleon of a uniform system of nucleons, expressed as a function of:

nuclear density: $\rho = \rho_n + \rho_p$

isospin asymmetry: $\delta = \frac{\rho_n - \rho_p}{\rho_n + \rho_p} = \frac{N-Z}{A}$

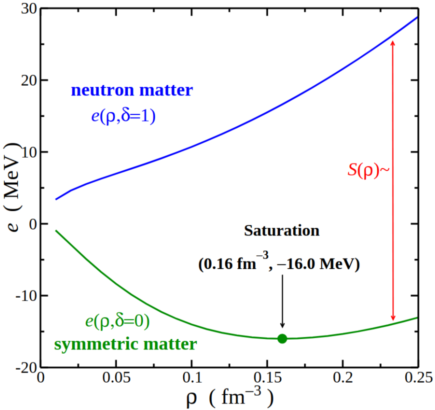

$$e(\rho, \delta) = e(\rho, \delta = 0) + S(\rho)\delta^2 + \ldots$$

Largest uncertainties on **symmetry energy** $S(\rho)$ term, customarily expanded around saturation density ρ_0:

$$S(\rho) = S(\rho_0) + L_{sym}x + \frac{1}{2}K_{sym}x^2 + \ldots$$

where $x = \frac{\rho - \rho_0}{3\rho_0}$

Astrophysics

Neutron star Mass-Radius relations via Tolman Oppenheimer-Volkoff eqn. NEoS represents a fundamental input.

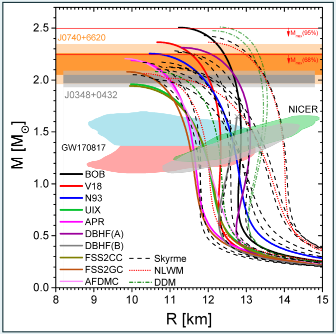

G.F. Burgio *et al.*, Symmetry 13(3), 400 (2021)

Observ.: NS masses/radii (→ NICER) +tidal deformability(→ GW)

Nuclear equation of state

Some observables in astrophysics and nuclear physics

Astrophysics

Neutron star Mass-Radius relations via Tolman Oppenheimer-Volkoff eqn. NEoS represents a fundamental input.

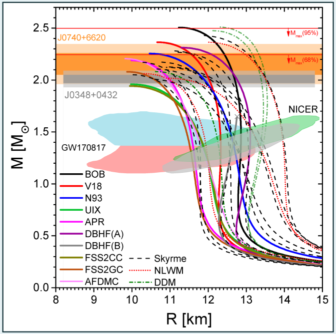

G.F. Burgio *et al.*, Symmetry 13(3), 400 (2021)

Observ.: NS masses/radii (→ NICER) +tidal deformability(→ GW)

Nuclear physics

Observ.: nuclear masses, neutron skin thickness, dipole polarizability, dynamical processes in HIC...

Astrophysics

Neutron star Mass-Radius relations via Tolman Oppenheimer-Volkoff eqn. NEoS represents a fundamental input.

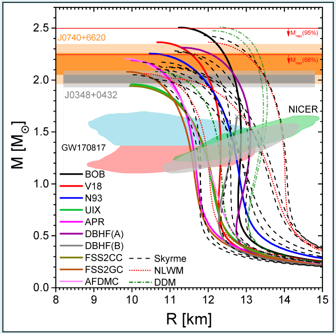

G.F. Burgio *et al.*, Symmetry 13(3), 400 (2021)

Observ.: NS masses/radii (→ NICER) +tidal deformability(→ GW)

Nuclear physics

Observ.: nuclear masses, neutron skin thickness, dipole polarizability, dynamical processes in HIC...

Isospin transport phenomena: sensitive probe to study $S(\rho)$

$$\mathbf{j}_n - \mathbf{j}_p \propto S(\rho)\nabla\delta + \delta\frac{\partial S(\rho)}{\partial\rho}\nabla\rho$$

Nuclear equation of state

Some observables in astrophysics and nuclear physics

Astrophysics

Neutron star Mass-Radius relations via Tolman Oppenheimer-Volkoff eqn. NEoS represents a fundamental input.

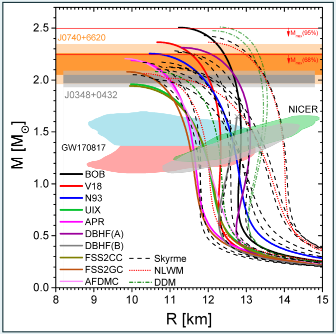

G.F. Burgio *et al.*, Symmetry 13(3), 400 (2021)

Observ.: NS masses/radii (→ NICER) +tidal deformability(→ GW)

Nuclear physics

Observ.: nuclear masses, neutron skin thickness, dipole polarizability, dynamical processes in HIC...

Isospin transport phenomena: sensitive probe to study $S(\rho)$

$$\mathbf{j}_n - \mathbf{j}_p \propto S(\rho)\nabla\delta + \delta\frac{\partial S(\rho)}{\partial\rho}\nabla\rho$$

Isospin diffusion: driven by isospin gradient in the system, leads to isospin equilibration.

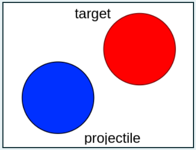

Nuclear equation of state

Some observables in astrophysics and nuclear physics

Astrophysics

Neutron star Mass-Radius relations via Tolman Oppenheimer-Volkoff eqn. NEoS represents a fundamental input.

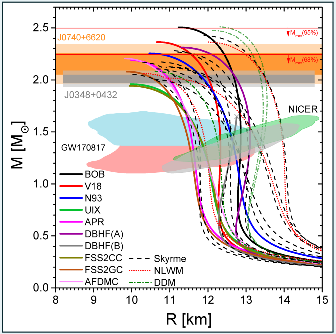

G.F. Burgio *et al.*, Symmetry 13(3), 400 (2021)

Observ.: NS masses/radii (→ NICER) +tidal deformability(→ GW)

Nuclear physics

Observ.: nuclear masses, neutron skin thickness, dipole polarizability, dynamical processes in HIC...

Isospin transport phenomena: sensitive probe to study $S(\rho)$

$$\mathbf{j}_n - \mathbf{j}_p \propto S(\rho)\nabla\delta + \delta\frac{\partial S(\rho)}{\partial\rho}\nabla\rho$$

Isospin diffusion: driven by isospin gradient in the system, leads to isospin equilibration.

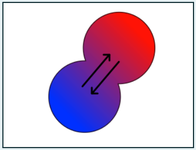

Nuclear equation of state

Some observables in astrophysics and nuclear physics

Astrophysics

Neutron star Mass-Radius relations via Tolman Oppenheimer-Volkoff eqn. NEoS represents a fundamental input.

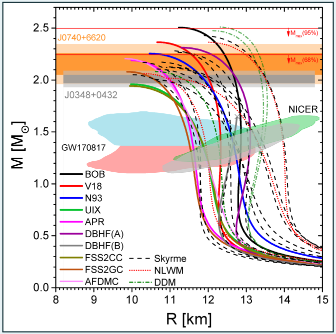

G.F. Burgio *et al.*, Symmetry 13(3), 400 (2021)

Observ.: NS masses/radii (→ NICER) +tidal deformability(→ GW)

Nuclear physics

Observ.: nuclear masses, neutron skin thickness, dipole polarizability, dynamical processes in HIC...

Isospin transport phenomena: sensitive probe to study $S(\rho)$

$$\mathbf{j}_n - \mathbf{j}_p \propto S(\rho)\nabla\delta + \delta\frac{\partial S(\rho)}{\partial\rho}\nabla\rho$$

Isospin diffusion: driven by isospin gradient in the system, leads to isospin equilibration.

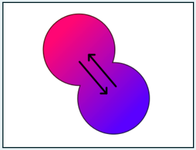

Astrophysics

Neutron star Mass-Radius relations via Tolman Oppenheimer-Volkoff eqn. NEoS represents a fundamental input.

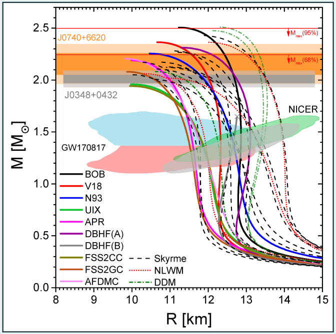

G.F. Burgio *et al.*, Symmetry 13(3), 400 (2021)

Observ.: NS masses/radii (→ NICER) +tidal deformability(→ GW)

Nuclear physics

Observ.: nuclear masses, neutron skin thickness, dipole polarizability, dynamical processes in HIC...

Isospin transport phenomena: sensitive probe to study $S(\rho)$

$$\mathbf{j}_n - \mathbf{j}_p \propto S(\rho)\nabla\delta + \delta\frac{\partial S(\rho)}{\partial\rho}\nabla\rho$$

Isospin diffusion: driven by isospin gradient in the system, leads to isospin equilibration.

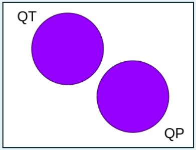

The INDRA-FAZIA setup

An eye on heavy ion collisions at Fermi energies

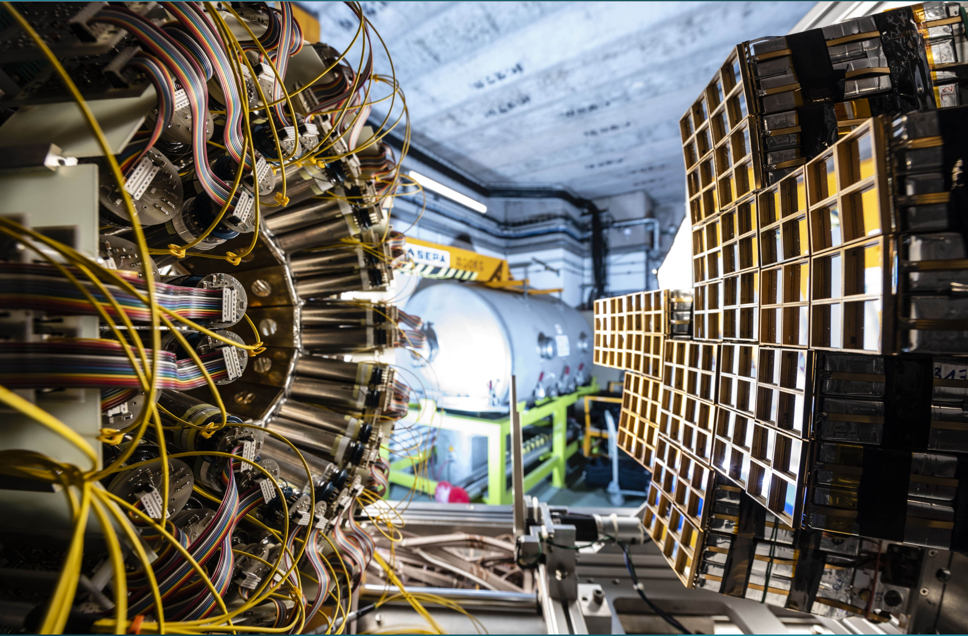

The INDRA-FAZIA setup

An eye on heavy ion collisions at Fermi energies

FAZIA

Forward-angle A and Z Identification Array

State of the art of ion identification in the Fermi energy domain

Designed to explore **isospin dynamics** in heavy ion collisions

Characteristics of portability, modularity, coupling capability

The INDRA-FAZIA setup

An eye on heavy ion collisions at Fermi energies

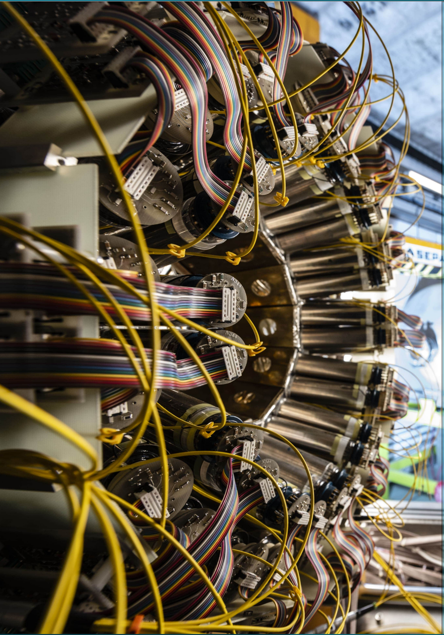

INDRA

Identification de Noyaux et Détection avec Résolutions Accrues

Offers large solid angle coverage (~80% of 4π) with high granularity

Provides a good global event reconstruction

Build global variables for reaction centrality estimation

INDRA

(Identification de Noyaux et Détection avec Résolutions Accrues)

- Original configuration made of 17 rings:
  - 1: Phoswich detectors
  - 2-9: Ionisation ch. + Si + CsI(Tl)
  - 10-17: Ionisation ch. + CsI(Tl)
- Charge discrimination up to uranium, mass discrimination up to $Z \sim 4$
  → Electronics upgrade (2020): now up to $Z \sim 10$
  J. D. Frankland et al., NIM A 1082 (2026) 170908
- Large solid angle coverage (90%) with high granularity (336 modules)

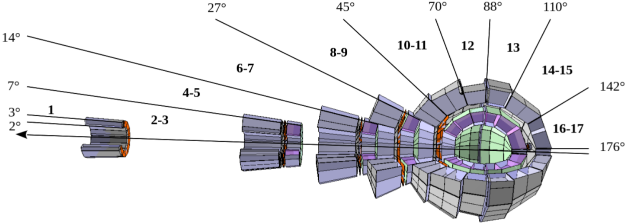

The FAZIA setup

An overview of the characteristics

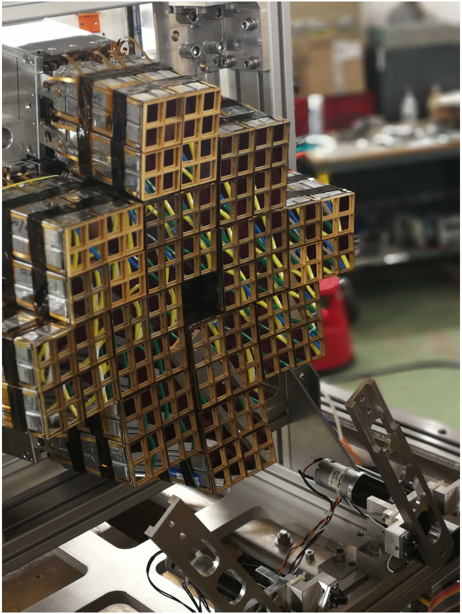

FAZIA

(Forward-angle A and Z Identification Array)

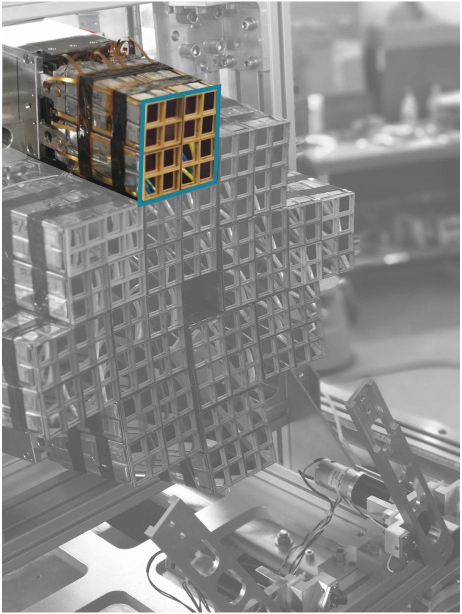

FAZIA
(Forward-angle A and Z Identification Array)

Basic module → **block**
made of 16 three-stage **telescopes**
($2 \times 2\,\text{cm}^2$ active area):

- Si1 300 μm thick
- Si2 500 μm (or 750 μm) thick
- CsI(Tl) 10cm thick

R. Bougault et al., Eur. Phys. J. A 50, 47 (2014)

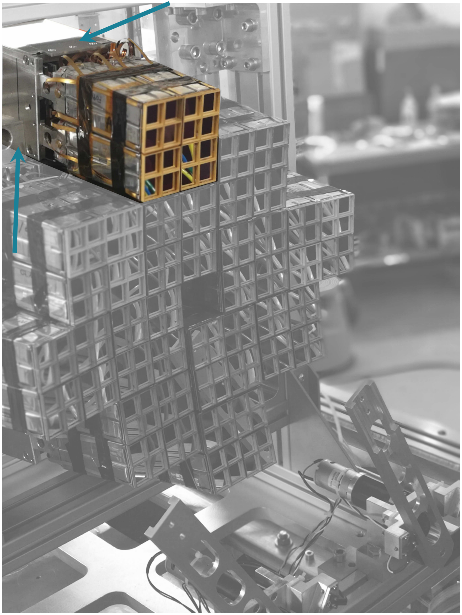

FAZIA

(Forward-angle A and Z Identification Array)

Basic module → **block**
made of 16 three-stage **telescopes**
($2 \times 2\,\mathrm{cm}^2$ active area):

- Si1 300 μm thick
- Si2 500 μm (or 750 μm) thick
- CsI(Tl) 10cm thick

R. Bougault et al., Eur. Phys. J. A 50, 47 (2014)

+ read-out electronics for all telescopes
S. Valdré et al., NIM A 930, 27 (2019)

Mass identification for different techniques:

- PSA in Si1: up to $Z \sim 22$
- ΔE-E in Si1-Si2: up to $Z \sim 25$
- ΔE-E in Si2-CsI: up to $Z \sim 27$ after upgrade with thicker Si2 (750 μm)
- PSA in CsI: up to $Z \sim 3$

Low identification thresholds (~ 1 MeV/nucl.) with PSA.

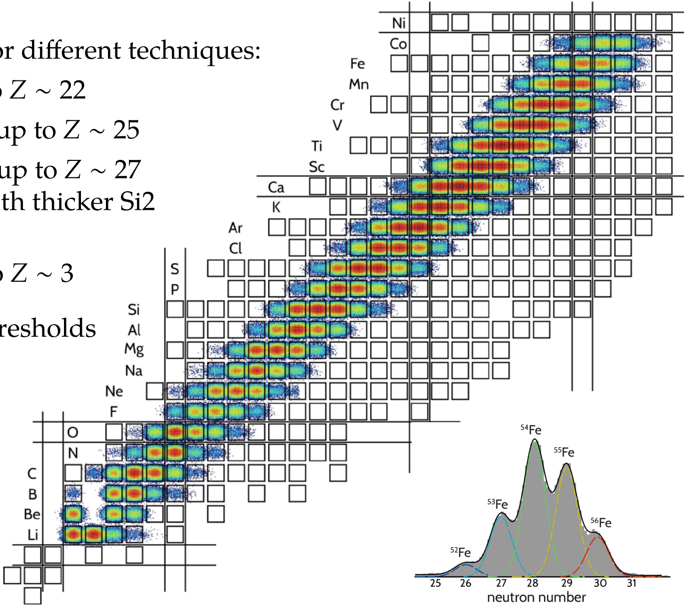

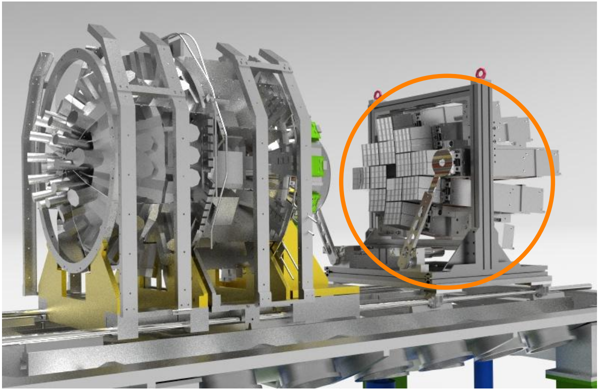

March 2019 → *Completion of the coupling of the two apparatuses*

- 12 FAZIA blocks cover forward polar angles (first 5 INDRA rings removed)

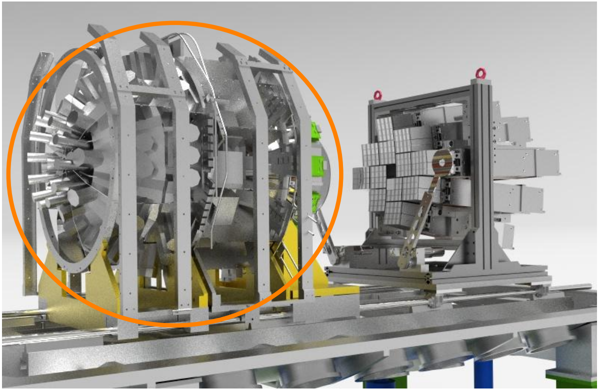

March 2019 → *Completion of the coupling of the two apparatuses*

- 12 FAZIA blocks cover forward polar angles (first 5 INDRA rings removed)
- The remaining part of INDRA (rings 6-17) covers the polar angles between 14° and 176° (∼ 80% of the 4π solid angle)

INDRA-FAZIA E789

First experimental campaign in GANIL (2019)

April-May 2019 → *first experiment exploiting the coupled INDRA-FAZIA setup*

INDRA-FAZIA E789 dataset → ^{58,64}Ni+^{58,64}Ni at 32 MeV/nucl.

Exp. aimed to study the **isospin diffusion mechanism** by comparing the products of the two asymmetric reactions with both the n-rich and n-deficient symmetric systems.
C.C. *et al.*, PRC 106, 024603 (2022), PRC 108, 054611 (2023), PRC 111, 044601 (2025), PLB 868 (2025) 139815

- **FAZIA** provides the direct information on the isospin content of the QP remnant
- **INDRA** allows for a model-independent assessment of the reaction centrality

INDRA-FAZIA E789
First experimental campaign in GANIL (2019)

April-May 2019 → *first experiment exploiting the coupled INDRA-FAZIA setup*

INDRA-FAZIA E789 dataset → ^{58,64}Ni+^{58,64}Ni at 32 MeV/nucl.

Exp. aimed to study the **isospin diffusion mechanism** by comparing the products of the two asymmetric reactions with both the n-rich and n-deficient symmetric systems.
C.C. *et al.*, PRC 106, 024603 (2022), PRC 108, 054611 (2023), PRC 111, 044601 (2025), PLB 868 (2025) 139815

- **FAZIA** provides the direct information on the isospin content of the QP remnant
- **INDRA** allows for a model-independent assessment of the reaction centrality

INDRA 2nd camp. dataset → ^{58}Ni+^{58}Ni at 32 MeV/nucl.

Minimum bias trigger condition, suitable for the application of the *impact parameter reconstruction method* of J. D. Frankland *et al.*, Phys. Rev. C 104, 034609 (2021)

⇒ combined analysis of the two datasets

n.b. important role of $M-b$ intrinsic fluctuations to be taken into account

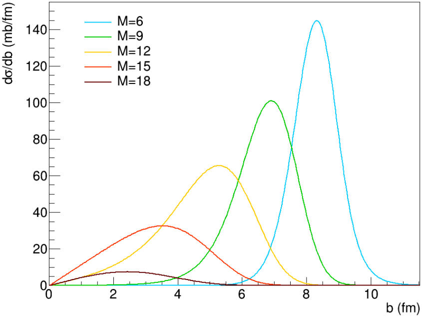

Model-independent ⟨N/Z⟩ for the QP remnant as a function of b for the four systems in the INDRA-FAZIA dataset
→ clear effect of isospin equilibration

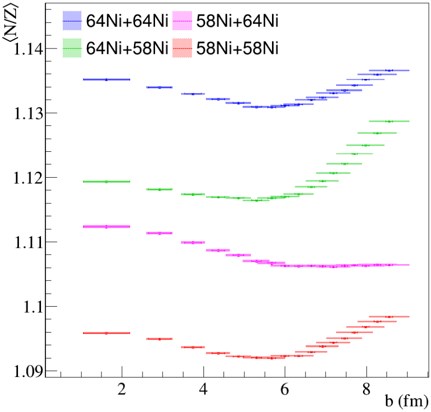

Model-independent ⟨N/Z⟩ for the QP remnant as a function of b for the four systems in the INDRA-FAZIA dataset
→ clear effect of isospin equilibration

Isospin transport ratio: highlights isospin diffusion effect, bypassing the effects acting similarly on the four systems

F. Rami et al., Phys. Rev. Lett. 84, 1120 (2000)

$$R(x) = \frac{2x_i - x_{AA} - x_{BB}}{x_{AA} - x_{BB}}$$

where x is an isospin sensitive observable ($\langle N/Z \rangle$), $A = ^{64}$Ni, $B = ^{58}$Ni and $i = AA, AB, BA, BB$.

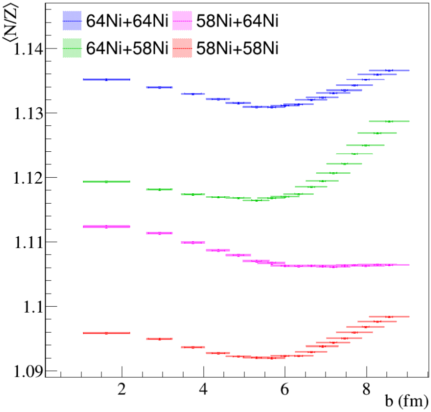

Model-independent ⟨N/Z⟩ for the QP remnant as a function of b for the four systems in the INDRA-FAZIA dataset
→ clear effect of isospin equilibration

Isospin transport ratio: highlights isospin diffusion effect, bypassing the effects acting similarly on the four systems

F. Rami et al., Phys. Rev. Lett. 84, 1120 (2000)

$$R(x) = \frac{2x_i - x_{AA} - x_{BB}}{x_{AA} - x_{BB}}$$

where x is an isospin sensitive observable ($\langle N/Z \rangle$), $A = {}^{64}$Ni, $B = {}^{58}$Ni and $i = AA, AB, BA, BB$.

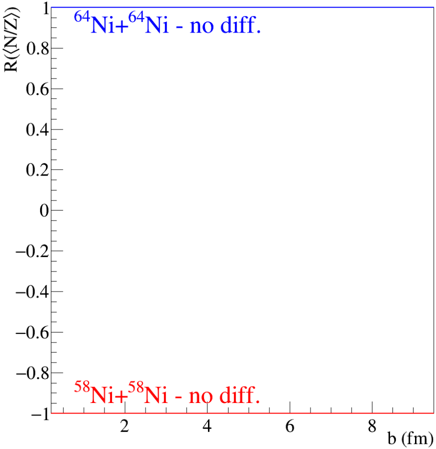

Model-independent ⟨N/Z⟩ for the QP remnant as a function of b for the four systems in the INDRA-FAZIA dataset
→ clear effect of isospin equilibration

Isospin transport ratio: highlights isospin diffusion effect, bypassing the effects acting similarly on the four systems

F. Rami et al., Phys. Rev. Lett. 84, 1120 (2000)

$$R(x) = \frac{2x_i - x_{AA} - x_{BB}}{x_{AA} - x_{BB}}$$

where x is an isospin sensitive observable ($\langle N/Z \rangle$), $A = ^{64}$Ni, $B = ^{58}$Ni and $i = AA, AB, BA, BB$.

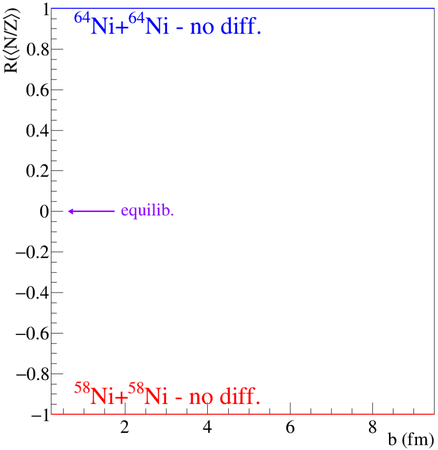

Model-independent ⟨N/Z⟩ for the QP remnant as a function of b for the four systems in the INDRA-FAZIA dataset
→ clear effect of isospin equilibration

Isospin transport ratio: highlights isospin diffusion effect, bypassing the effects acting similarly on the four systems

F. Rami et al., Phys. Rev. Lett. 84, 1120 (2000)

$$R(x) = \frac{2x_i - x_{AA} - x_{BB}}{x_{AA} - x_{BB}}$$

where x is an isospin sensitive observable ($\langle N/Z \rangle$), $A = ^{64}$Ni, $B = ^{58}$Ni and $i = AA$, AB, BA, BB.

Model-independent $R(\langle N/Z \rangle_{QPr})$ as a function of the impact parameter b
→ experimental reference for comparison with theoretical predictions from transport models

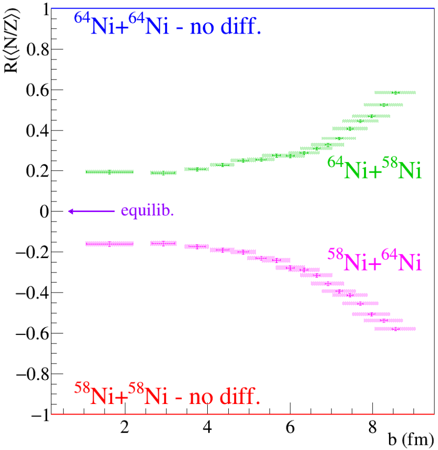

C. Ciampi *et al.*, Phys. Rev. C 111, 044601 (2025)

Comparison between the experimental $R(\langle N/Z\rangle_{QPr})$ and the one predicted for *primary fragments* by transport code.

A. Camaiani *et al.*, Phys. Rev. C 102, 044607 (2020)
S. Mallik *et al.*, J. Phys. G 49, 015102 (2021)

INDRA-FAZIA E789

Transport model simulations

Comparison between the experimental $R(\langle N/Z \rangle_{QPr})$ and the one predicted for *primary fragments* by transport code.

A. Camaiani *et al.*, Phys. Rev. C 102, 044607 (2020)
S. Mallik *et al.*, J. Phys. G 49, 015102 (2021)

Simulations carried out with the BUU@VECC-McGill transport code.

S. Mallik *et al.*, Phys. Rev. C 91, 034616 (2015)

NEoS parametrizations from *ab initio* and phenomenological approaches:

- *Ab initio*: two extreme χ-EFT interact., C. Drischler *et al.*, PRC 93, 054314 (2016)
- Phenomenological approaches:
  - SAMI (Skyrme), X. Roca-Maza *et al.*, Phys. Rev. C 86, 031306(R) (2012)
  - SGII (Skyrme), Nguyen Van Giai *et al.*, Phys. Lett. B106, 379 (1981)
  - NL3 (RMF), G. A. Lalazissis *et al.*, Phys. Rev. C 55, 540 (1997)

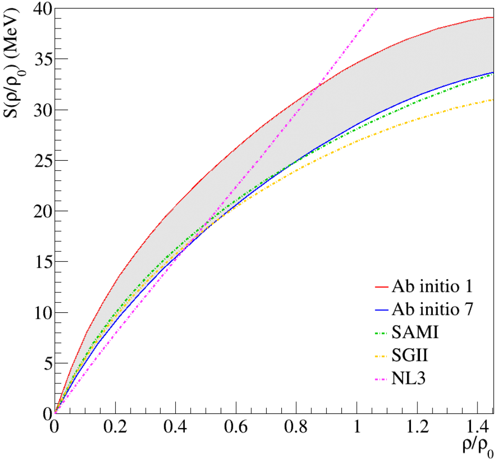

Comparison between the experimental $R(\langle N/Z \rangle_{QPr})$ and the one predicted for *primary fragments* by transport code.

A. Camaiani *et al.*, Phys. Rev. C 102, 044607 (2020)
S. Mallik *et al.*, J. Phys. G 49, 015102 (2021)

Simulations carried out with the BUU@VECC-McGill transport code.

S. Mallik *et al.*, Phys. Rev. C 91, 034616 (2015)

NEoS parametrizations from *ab initio* and phenomenological approaches:

- *Ab initio*: two extreme χ-EFT interact., C. Drischler *et al.*, PRC 93, 054314 (2016)
- Phenomenological approaches:
  - SAMI (Skyrme), X. Roca-Maza *et al.*, Phys. Rev. C 86, 031306(R) (2012)
  - SGII (Skyrme), Nguyen Van Giai *et al.*, Phys. Lett. B106, 379 (1981)
  - NL3 (RMF), G. A. Lalazissis *et al.*, Phys. Rev. C 55, 540 (1997)

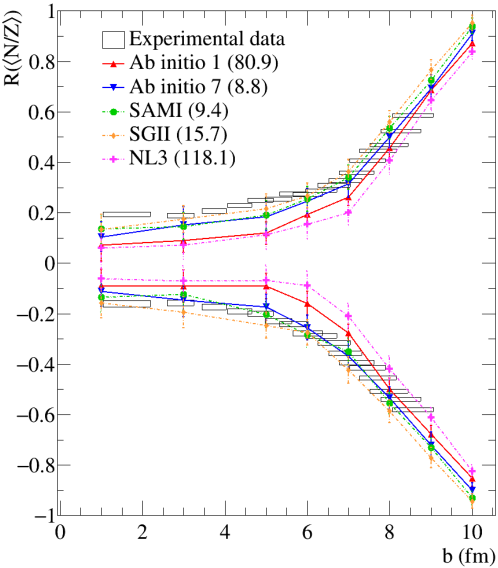

A more quantitative analysis using the χ^2 values:

- $\chi^2(S(\rho/\rho_0))$ extracted via quadratic fit at each ρ/ρ_0
- We assume a gaussian likelihood along $S(\rho/\rho_0)$:

$$\mathcal{L}(S(\rho/\rho_0)) \propto e^{-\chi^2(S(\rho/\rho_0))/2}$$

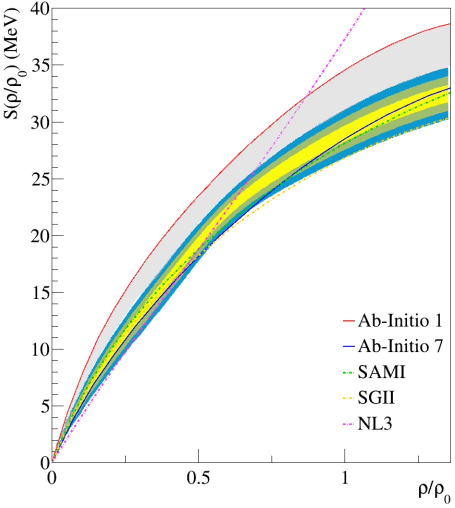

A more quantitative analysis using the χ^2 values:

- $\chi^2(S(\rho/\rho_0))$ extracted via quadratic fit at each ρ/ρ_0
- We assume a gaussian likelihood along $S(\rho/\rho_0)$:

$$\mathcal{L}(S(\rho/\rho_0)) \propto e^{-\chi^2(S(\rho/\rho_0))/2}$$

⚠ Not all density regions are equivalently probed by considering isospin diffusion

→ define a *weight function* to account for the sensitive density region

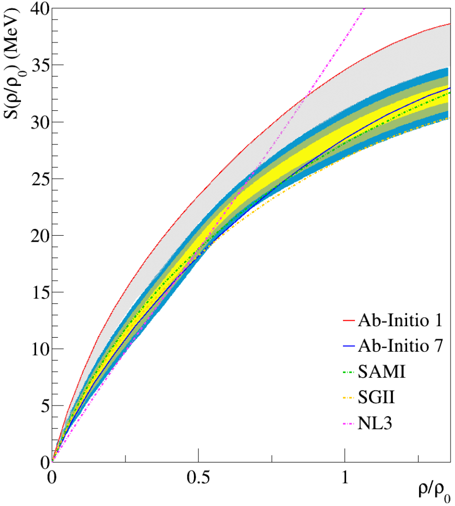

Study of the evolution of **baryonic density** and **isospin current density** extracted from BUU@VECC-McGill.
(quantities evaluated for *ab initio* 7 param. over $r = 3$ fm spherical volume)

n.b. maximum exchange found in the compression phase (highest densities)

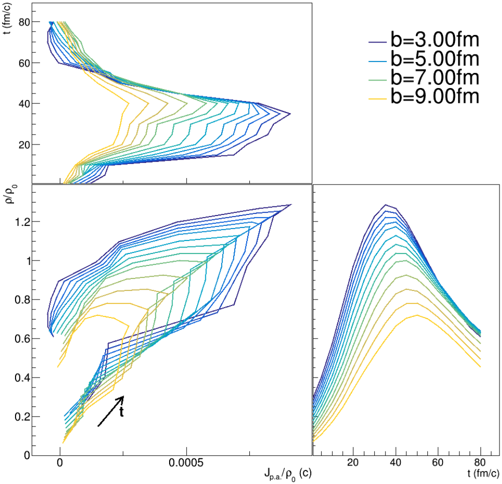

INDRA-FAZIA E789

Sensitive density region: study of isospin current and baryonic densities

Study of the evolution of **baryonic density** and **isospin current density** extracted from BUU@VECC-McGill.
(quantities evaluated for *ab initio 7* param. over $r = 3$ fm spherical volume)

n.b. maximum exchange found in the compression phase (highest densities)

Weight function for a given b:

$$w_b(\rho/\rho_0) = \int_{t_{\mathrm{start}}}^{t_{\mathrm{stop}}} j_{\mathrm{p.a.}}(t)\, \delta(\rho/\rho_0 - \rho(t)/\rho_0)\, dt$$

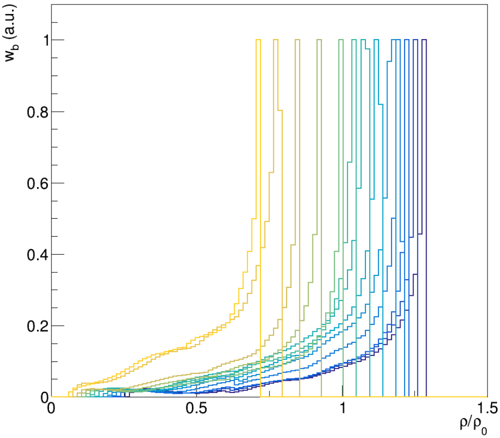

Study of the evolution of **baryonic density** and **isospin current density** extracted from BUU@VECC-McGill.
(quantities evaluated for *ab initio* 7 param. over $r = 3$ fm spherical volume)

n.b. maximum exchange found in the compression phase (highest densities)

Weight function for a given b:

$$w_b(\rho/\rho_0) = \int_{t_{\mathrm{start}}}^{t_{\mathrm{stop}}} j_{\mathrm{p.a.}}(t)\,\delta(\rho/\rho_0 - \rho(t)/\rho_0)\,dt$$

Global weight function $w(\rho/\rho_0)$:

$$w(\rho/\rho_0) = \int_{b_{\mathrm{min}}}^{b_{\mathrm{max}}} \tilde{w}_b(\rho/\rho_0)\,db$$

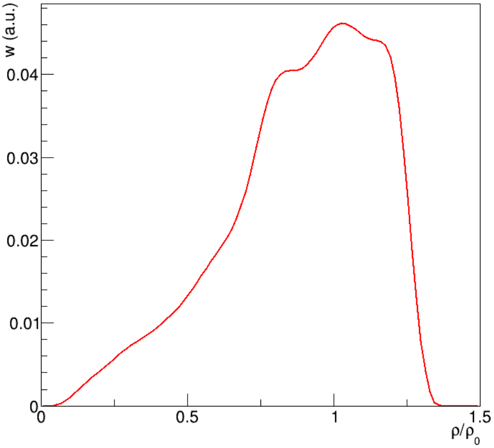

Confidence regions $1\sigma, 2\sigma, 3\sigma$ defined based on weighted $\mathcal{L}(S(\rho/\rho_0))$:

- Sensitivity close to saturation - anticipated by NL3 rejection, different from SAMI, SGII, AI7 for $\rho > 0.5\rho_0$

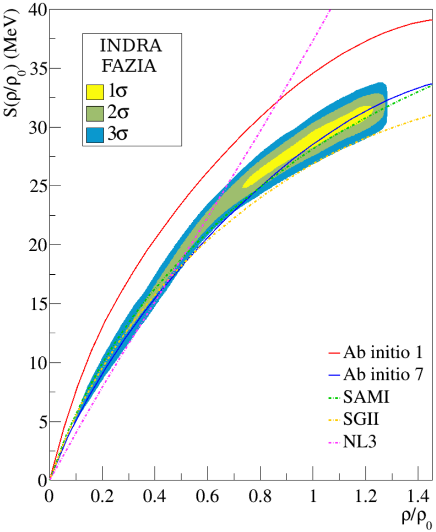

C. Ciampi *et al.*, Phys. Lett. B 868 (2025) 139815

Confidence regions $1\sigma, 2\sigma, 3\sigma$ defined based on weighted $\mathcal{L}(S(\rho/\rho_0))$:

- Sensitivity close to saturation - anticipated by NL3 rejection, different from SAMI, SGII, AI7 for $\rho > 0.5\rho_0$
- Good agreement with χ-EFT - towards the softer side of its uncertainty band

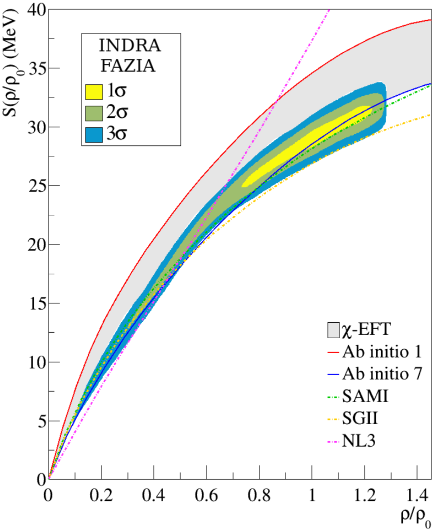

C. Ciampi *et al.*, Phys. Lett. B 868 (2025) 139815

Confidence regions $1\sigma, 2\sigma, 3\sigma$ defined based on weighted $\mathcal{L}(S(\rho/\rho_0))$:

- Sensitivity close to saturation - anticipated by NL3 rejection, different from SAMI, SGII, AI7 for $\rho > 0.5\rho_0$
- Good agreement with χ-EFT - towards the softer side of its uncertainty band
- Good agreement with isospin diffusion data in Sn+Sn collisions (but we declare a different ρ sensitivity)

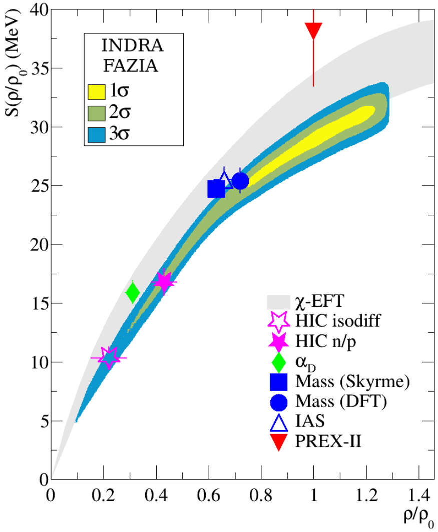

W. G. Lynch *et al.*, Phys. Lett. B 830, 137098 (2022).
M. B. Tsang *et al.*, Phys. Rev. Lett. 102, 122701 (2009).
P. Morfouace *et al.*, Phys. Lett. B 799, 135045 (2019).
Z. Zhang *et al.*, Phys. Rev. C 92, 031301R (2015).
M. Kortelainen *et al.*, Phys. Rev. C 85, 024304 (2012).
P. Danielewicz *et al.*, Nucl. Phys. A 958, 147 (2017).
B. T. Reed *et al.*, Phys. Rev. Lett. 126, 172503 (2021).

C. Ciampi *et al.*, Phys. Lett. B 868 (2025) 139815

Description of nuclear matter at low density and finite temperature:

- Need to account for **light cluster** formation and the in-medium effects on their properties

S. Typel *et al.*, Phys. Rev. C 81, 015803 (2010)

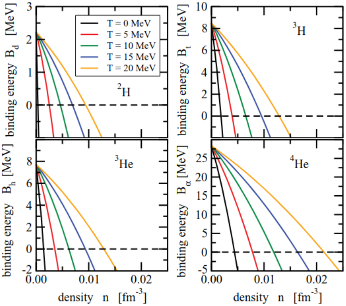

Description of nuclear matter at low density and finite temperature:

- Need to account for **light cluster** formation and the in-medium effects on their properties
  S. Typel *et al.*, Phys. Rev. C 81, 015803 (2010)
- Necessary ingredient for astrophysical models
  (e.g. shock wave dynamics in core-collapse supernovae, size of nucleosynthesis seeds in NS mergers, proto-NS cooling...)
  T. Fischer *et al.*, Eur. Phys. J. A (2014) 50: 46

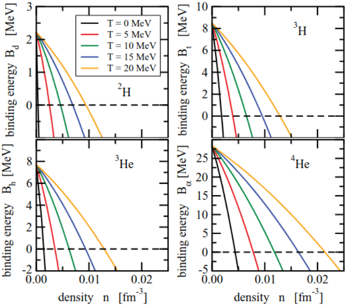

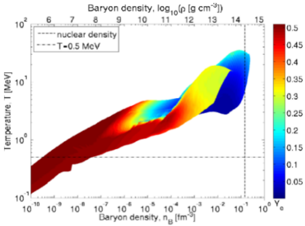

Description of nuclear matter at low density and finite temperature:

- Need to account for **light cluster** formation and the in-medium effects on their properties
  S. Typel *et al.*, Phys. Rev. C 81, 015803 (2010)
- Necessary ingredient for astrophysical models
  (e.g. shock wave dynamics in core-collapse supernovae, size of nucleosynthesis seeds in NS mergers, proto-NS cooling...)
  T. Fischer *et al.*, Eur. Phys. J. A (2014) 50: 46

Central HICs → gas of protons, neutrons, clusters

- Need to consider in-medium effects
  L. Qin *et al.*, Phys. Rev. Lett. 108, 172701 (2012)

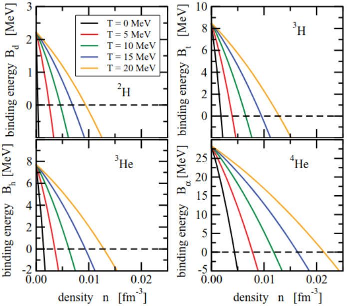

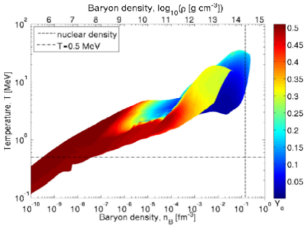

Description of nuclear matter at low density and finite temperature:

- Need to account for **light cluster** formation and the in-medium effects on their properties
  S. Typel *et al.*, Phys. Rev. C 81, 015803 (2010)
- Necessary ingredient for astrophysical models
  (e.g. shock wave dynamics in core-collapse supernovae, size of nucleosynthesis seeds in NS mergers, proto-NS cooling...)
  T. Fischer *et al.*, Eur. Phys. J. A (2014) 50: 46

Central HICs → gas of protons, neutrons, clusters

- Need to consider in-medium effects
  L. Qin *et al.*, Phys. Rev. Lett. 108, 172701 (2012)
- Xe+Sn at 32MeV/nucl. INDRA data → T, ρ estimate vs Coulomb-corrected part. velocity
  R. Bougault *et al.*, J. Phys. G 47, 025103 (2020)

Angular selection : mid-velocity products

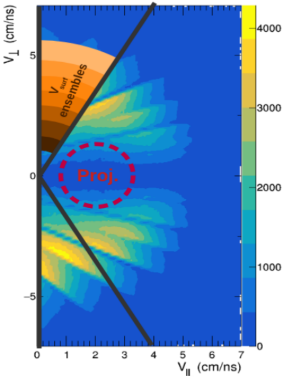

Description of nuclear matter at low density and finite temperature:

- Need to account for **light cluster** formation and the in-medium effects on their properties
  S. Typel *et al.*, Phys. Rev. C 81, 015803 (2010)
- Necessary ingredient for astrophysical models
  (e.g. shock wave dynamics in core-collapse supernovae, size of nucleosynthesis seeds in NS mergers, proto-NS cooling...)
  T. Fischer *et al.*, Eur. Phys. J. A (2014) 50: 46

Central HICs → gas of protons, neutrons, clusters

- Need to consider in-medium effects
  L. Qin *et al.*, Phys. Rev. Lett. 108, 172701 (2012)
- Xe+Sn at 32MeV/nucl. INDRA data → T, ρ estimate vs Coulomb-corrected part. velocity
  R. Bougault *et al.*, J. Phys. G 47, 025103 (2020)
- $K_c = \frac{\rho(A,Z)}{\rho_p^Z \rho_n^{(A-Z)}}$ comparison with RMF prediction
  → calibration of the in-medium modification of the cluster-σ coupling $g_{\sigma j} = x_s A_j g_{\sigma N}$
  H. Pais *et al.*, Phys. Rev. Lett. 125, 012701 (2020)

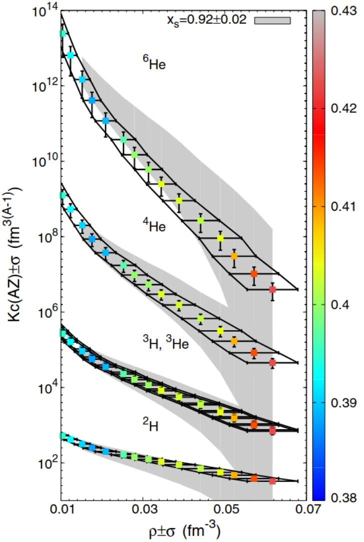

New approach to avoid ideal gas assumption:
full Bayesian inference with RMF predictions

- Inference based on direct observables:
  measured mass fractions $\omega_{AZ} = AY_{AZ}/A_T$

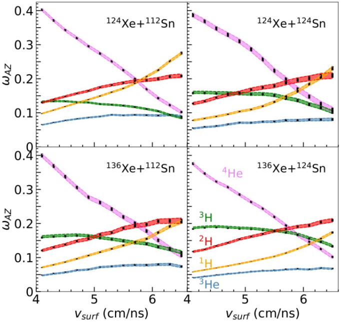

New approach to avoid ideal gas assumption:
full Bayesian inference with RMF predictions

- Inference based on direct observables:
  measured mass fractions $\omega_{AZ} = AY_{AZ}/A_T$
- Out: posterior distributions of T, ρ and $x_s(\rho, T)$

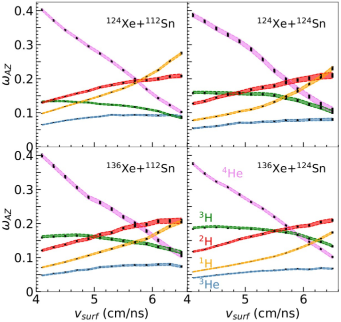

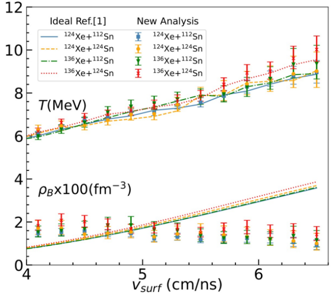

New approach to avoid ideal gas assumption:
full Bayesian inference with RMF predictions

- Inference based on direct observables: measured mass fractions $\omega_{AZ} = AY_{AZ}/A_T$
- Out: posterior distributions of T, ρ and $x_s(\rho, T)$
  $\Rightarrow$ Evolution of x_s with temperature

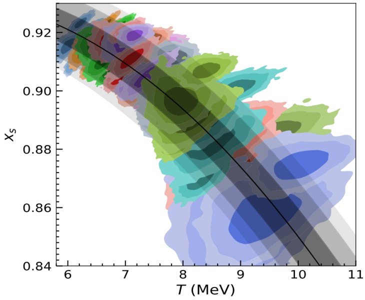

New approach to avoid ideal gas assumption:
full Bayesian inference with RMF predictions

- Inference based on direct observables: measured mass fractions $\omega_{AZ} = AY_{AZ}/A_T$
- Out: posterior distributions of T, ρ and $x_s(\rho, T)$
  $\Rightarrow$ Evolution of x_s with temperature
- Consequence on the total cluster abundance evolution with T

T. Custodio *et al.*, Phys. Rev. Lett. 134, 082304 (2025)

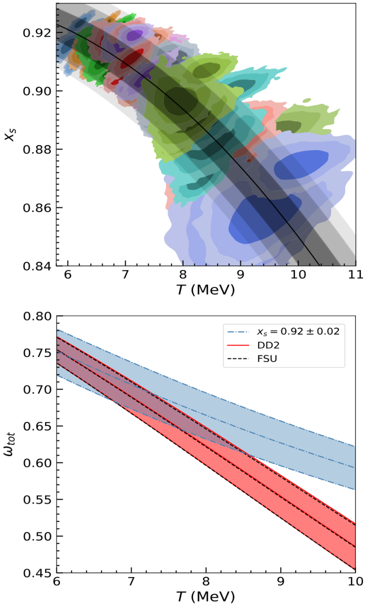

New approach to avoid ideal gas assumption: **full Bayesian inference** with RMF predictions

- Inference based on direct observables: measured mass fractions $\omega_{AZ} = AY_{AZ}/A_T$
- Out: posterior distributions of T, ρ and $x_s(\rho, T)$ $\Rightarrow$ Evolution of x_s with temperature
- Consequence on the total cluster abundance evolution with T

T. Custodio *et al.*, Phys. Rev. Lett. 134, 082304 (2025)

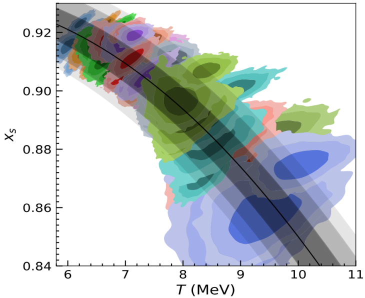

"Extending our knowledge of warm dense nuclear matter in the low density region"

R. Bougault, G. Casini *et al.*, E818 proposal, GANIL PAC 2020

- INDRA-FAZIA exp. at GANIL in 2022: ^{36}Ar,^{58}Ni+^{58}Ni at 74 MeV/nucl.
- Analysis of the QP vaporization source
- Extend the analysis to heavier clusters

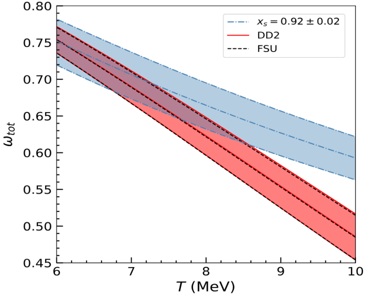

INDRA-FAZIA 2025 campaign

E884: Isospin transport in QP breakup events

"Impact of projectile-target asymmetry on the isospin equilibration rate extracted from QP breakup reactions"

C. Ciampi, J. D. Frankland *et al.*, E884 proposal, GANIL PAC 2023

- Study of the interplay between isospin drift and diffusion in the QP dynamical fission channel
- ^{70}Zn+^{27}Al,^{70}Zn,^{209}Bi at 35 MeV/nucl.

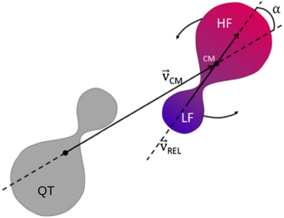

Extraction of isospin equilibration rate:

- Angle α between QP-QT separation axis and QP fission axis interpreted as a clock for breakup timescale
  A. Jedele *et al.*, Phys. Rev. Lett. 118, 062501 (2017)
- Evolution of isospin content of breakup fragments vs α → isosp. equilibration rate

Data reduction to be completed.

Preliminary results already show a clear effect of isospin equilibration with α.

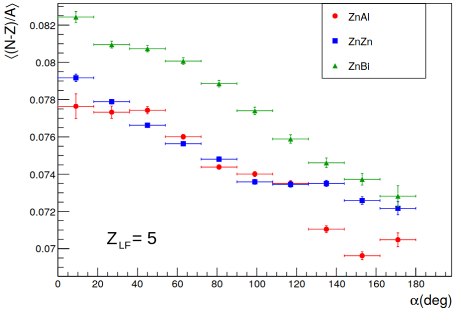

G. Naddeo, Master's thesis, *Università di Napoli Federico II* (2025); B. Gnoffo, GANIL visiting scientist 2026

"Measurement of the Hoyle state radius via inelastic scattering of ^{12}C+^{12}C at 8.75 MeV/nucleon"

D. Gruyer, D. Dell'Aquila *et al.*, E881 proposal, GANIL PAC 2023

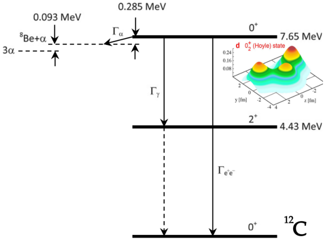

- **^{12}C Hoyle state**: second excited 0^+ state at 7.65 MeV, crucial for stellar nucleosynthesis.
- Strong α-cluster character, but with different predictions on the spatial configuration and on the radius.

Charged particle spectroscopy on multi-α coincidence measurements.

- Invariant mass method on 3α
  $\rightarrow E^*$ of ^{12}C(proj)
- Missing mass method on recon. proj.
  $\rightarrow E^*$ of ^{12}C(targ)
  $\Rightarrow$ selection of E^* combinations

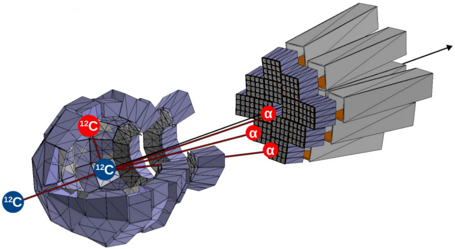

$\rightarrow$ *see talk by **Ilham Dekhissi** (05/11, 14h40)*

I. Dekhissi, PhD thesis, *Université de Caen* (2027); A. De Rosa, Master's thesis, *Università di Napoli Federico II* (2025)

Some perspectives

Upcoming experiment E894: α-clustering in neutron-rich oxygen isotopes

"α-clustering in neutron-rich oxygen isotopes"

J. Benlliure, A. Chbihi *et al.*, E894 proposal, GANIL PAC 2024

- Aimed at understanding the interplay between α-cluster formation and neutron skin
    - α-clusters expected at low-density surface region
    - n-skin formation can suppress α clusterization

      J.Tanaka *et al.*, Science 371, 260-264 (2021).
- Role of clustering in the relationship between the neutron-skin thickness and the L_{sym} parameter of the symmetry energy.

Study of α-transfer reaction cross section along the oxygen isotopic chain:

- (d,^{6}Li) reactions induced by ^{16,18,20}O beams at 7.5 MeV/nucl.
- Unambiguous determination of reaction channel thanks to multi-hit identification capability

  → study of cluster configurations of unbound states of O isotopes populated by inelastic reactions

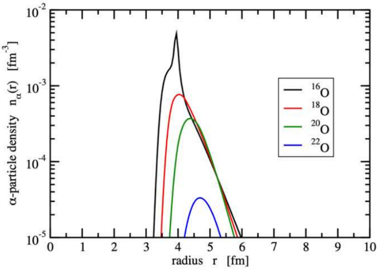

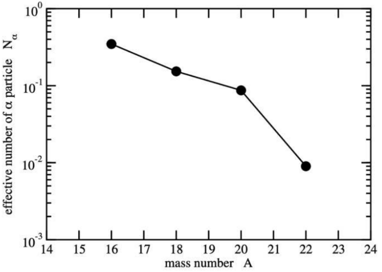

S. Typel, *private communication*

Some perspectives

Exploiting FAZIA's portability, modularity, coupling capability

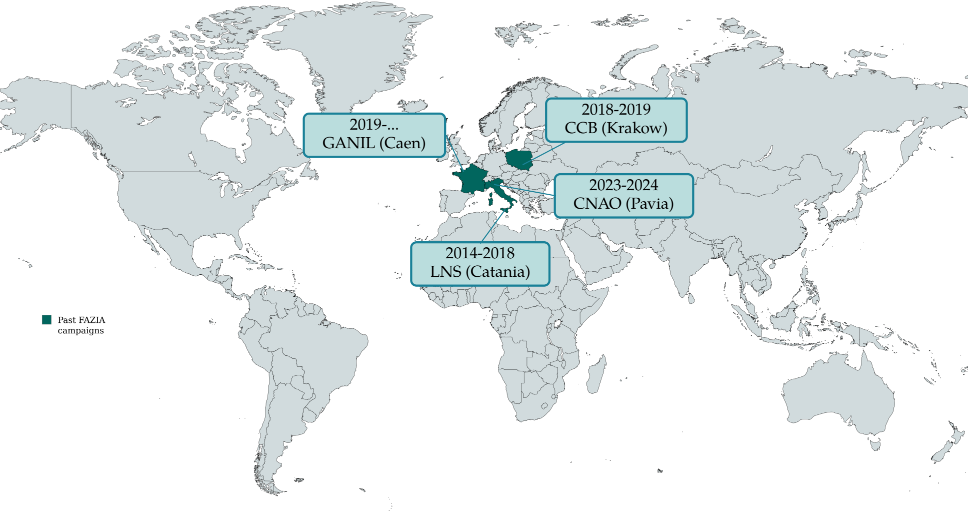

Some perspectives

Exploiting FAZIA's portability, modularity, coupling capability

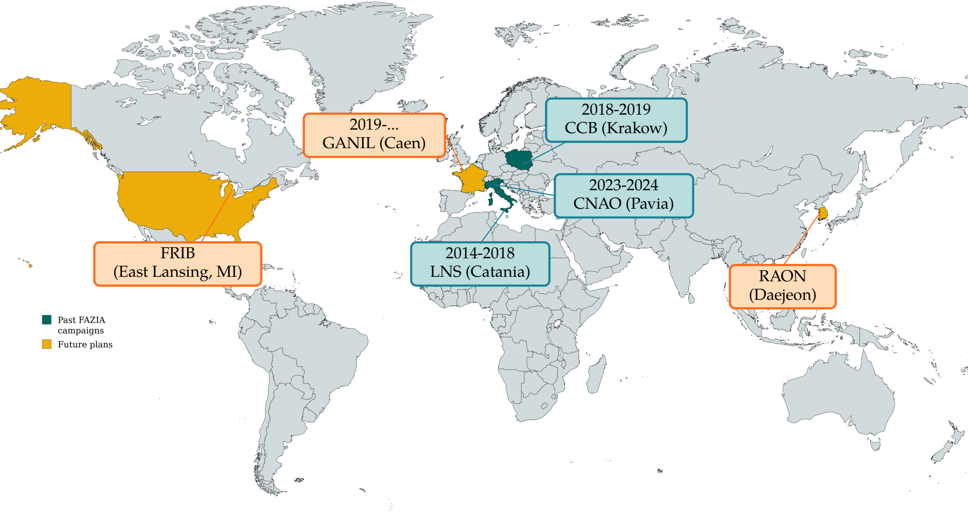

Thank you!

INDRA FAZIA

S. Barlini, D. Gruyer, G. Casini, N. Le Neindre, L. Baldesi, B. Borderie, R. Bougault, A. Camaiani, A. Chbihi, **C. Ciampi**, I. Dekhissi, D. Dell'Aquila, J. A. Dueñas, Q. Fable, J. D. Frankland, F. Gramegna, M. Henri, B. Hong, S. Kim, A. Kordyasz, T. Kozik, I. Lombardo, O. Lopez, T. Marchi, S. H. Nam, J. Park, M. Pârlog, G. Pasquali, S. Piantelli, G. Poggi, A. Rebillard-Soulié, S. Valdré, G. Verde, E. Vient

Collaborators:
F. Gulminelli, S. Mallik, T. Custodio, H. Pais, T. Malik, C. Providencia

Backup slides

Impact parameter reconstruction

Basic structure of the method

Centrality-related observable $X \longleftrightarrow$ deduce the correspondence with b

(see J. D. Frankland et al., PRC104, 034609 (2021), R. Rogly et al., PRC98, 024902 (2018))

$\Rightarrow$ Need to model the conditional probability distribution: $\mathbf{P}(\mathbf{X}|\mathbf{b})$

Step 1

Parametrize the $\mathbf{P}(\mathbf{X}|\mathbf{b})$, taking into account both the mean value and the fluctuations

Impact parameter reconstruction

Basic structure of the method

Centrality-related observable $X \longleftrightarrow$ deduce the correspondence with b

(see J. D. Frankland et al., PRC104, 034609 (2021), R. Rogly et al., PRC98, 024902 (2018))

$\Rightarrow$ Need to model the conditional probability distribution: $\mathbf{P(X|b)}$

Step 1

Parametrize the $\mathbf{P(X|b)}$, taking into account both the mean value and the fluctuations

Step 2

From the **inclusive** distribution $P(X)$, extract the $\mathbf{P(X|b)}$ parameters by fitting:

$$P(X) = \int_0^\infty P(b)\,\mathbf{P(X|b)}\,db \qquad P(b) = \frac{2\pi b}{1 + \exp\left(\frac{b-b_0}{\Delta b}\right)}$$

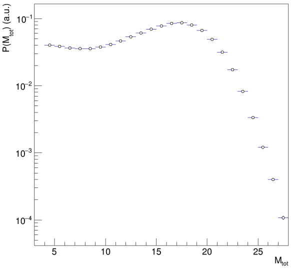

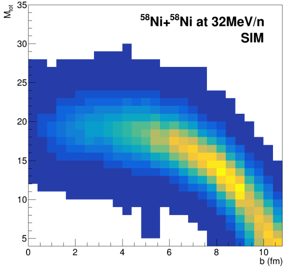

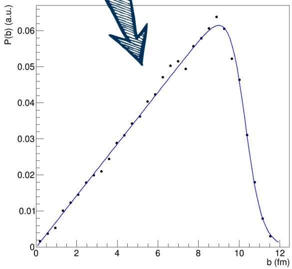

Impact parameter reconstruction

Basic structure of the method

Centrality-related observable $X \longleftrightarrow$ deduce the correspondence with b

(see J. D. Frankland et al., PRC104, 034609 (2021), R. Rogly et al., PRC98, 024902 (2018))

$\Rightarrow$ Need to model the conditional probability distribution: $\mathbf{P(X|b)}$

Step 1

Parametrize the $\mathbf{P(X|b)}$, taking into account both the mean value and the fluctuations

Step 2

From the **inclusive** distribution $P(X)$, extract the $\mathbf{P(X|b)}$ parameters by fitting:

$$P(X) = \int_0^{\infty} P(b)\,\mathbf{P(X|b)}\,db \qquad P(b) = \frac{2\pi b}{1 + \exp\left(\frac{b-b_0}{\Delta b}\right)}$$

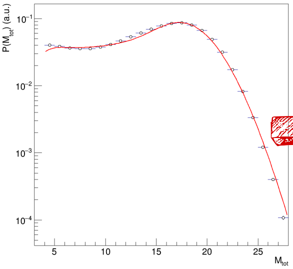

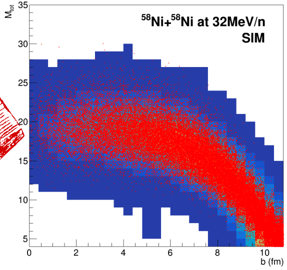

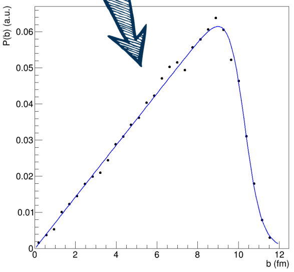

Impact parameter reconstruction

Basic structure of the method

Centrality-related observable $X \longleftrightarrow$ deduce the correspondence with b

(see J. D. Frankland et al., PRC104, 034609 (2021), R. Rogly et al., PRC98, 024902 (2018))

$\Rightarrow$ Need to model the conditional probability distribution: $\mathbf{P(X|b)}$

Step 1

Parametrize the $\mathbf{P(X|b)}$, taking into account both the mean value and the fluctuations

Step 2

From the **inclusive** distribution $P(X)$, extract the $\mathbf{P(X|b)}$ parameters by fitting:

$$P(X) = \int_0^{\infty} P(b)\,\mathbf{P(X|b)}\,db \qquad P(b) = \frac{2\pi b}{1 + \exp\left(\frac{b-b_0}{\Delta b}\right)}$$

Step 3

Having the $\mathbf{P(X|b)}$, for each X selection we can evaluate:

$$P(b|x_1 < X < x_2) = \frac{\int_{x_1}^{x_2} P(b,X)\,dX}{\int_{x_1}^{x_2} P(X)\,dX} = \frac{\int_{x_1}^{x_2} P(X)\,P(b|X)\,dX}{\int_{x_1}^{x_2} P(X)\,dX} = \frac{\int_{x_1}^{x_2} P(b)\,\mathbf{P(X|b)}\,dX}{\int_{x_1}^{x_2} P(X)\,dX}$$

⚠ To obtain the impact parameter distribution, it is necessary to perform the fit on the most inclusive $P(X)$ distribution, for which the $P(b)$ above can be assumed.

Impact parameter reconstruction

Detailed structure of the method

Given a centrality observable X, its inclusive distribution $P(X)$ can be expressed as:

$$P(X) = \int_0^{\infty} P(X,b)\,db = \int_0^{\infty} P(b)\,P(X|b)\,db = \int_0^{1} P(X|c_b)\,dc_b$$

where a change of variables is applied, introducing the centrality $c_b \equiv \int_0^b P(b')\,db'$ and exploiting that $P(c_b) = 1$.

Key step: model the $P(X|c_b)$ and extract its parameters by fitting the experimental $P(X)$

X assumes positive values $\rightarrow$ non-negative gamma distribution as fluctuation kernel:

$$P(X|c_b) = \frac{1}{\Gamma(k)\theta^k} X^{k-1}\, e^{-X/\theta} \qquad \text{where } \bar{X} = k\theta \text{ and } \sigma_X = \sqrt{k}\theta$$

where k and θ generally evolve with centrality. For them we assume:

- $k(c_b) = k_{\max}[1 - c_b^{\alpha}]^{\gamma} + k_{\min}$, where α, γ, $k_{\min}$ and $k_{\max}$ are parameters of the fit
- θ independent of centrality (problem is underconstrained) $\rightarrow$ θ is a fit parameter

Once the $P(X|c_b)$ is determined, one obtains:

$$P\left(c_b|x_1 \le X \le x_2\right) = \frac{\int_{x_1}^{x_2} P(c_b, X)\,dX}{\int_{x_1}^{x_2} P(X)\,dX} = \frac{\int_{x_1}^{x_2} P(X|c_b)\,dX}{\int_{x_1}^{x_2} P(X)\,dX}$$

and by changing back the variable: $P\left(b|x_1 \le X \le x_2\right) = P(b)\,P\left(c_b(b)|x_1 \le X \le x_2\right)$

Simulations carried out with the BUU@VECC-McGill transport code:

S. Mallik *et al.*, Phys. Rev. C 91, 034616 (2015)

- BUU code, setting 100 test particles/nucleon
- 8 impact parameters for each reaction/parametrization
- 200 events for each impact parameter/reaction/parametrization
- Simulation run until 300fm/c (ITR convergence)
- Possibility to plug in and test different nEoS via metamodeling technique

J. Margueron *et al.*, Phys. Rev. C 97, 025805 (2018)

	n_{sat} (fm^{-3})	E_{sat} (MeV)	E_{sym} (MeV)	L_{sym} (MeV)	K_{sat} (MeV)	K_{sym} (MeV)
Ab initio 1	0.189	-16.92	34.57	48.5	241	224
Ab initio 7	0.140	-13.23	28.53	43.9	43.9	-144
SAMI	0.1587	-15.93	28.16	43.7	245	-120
SGII	0.1583	-15.59	26.83	37.6	215	-146
NL3	0.1480	-16.24	37.35	118.3	271	101

Constraint on the nuclear EoS

Procedure for experimental-simulated data comparison

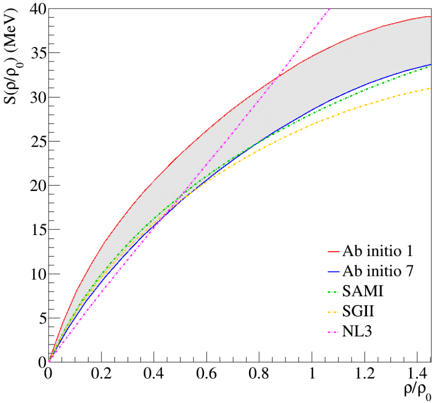

Constraint on the nuclear EoS
Procedure for experimental-simulated data comparison

At each value of ρ/ρ_0:

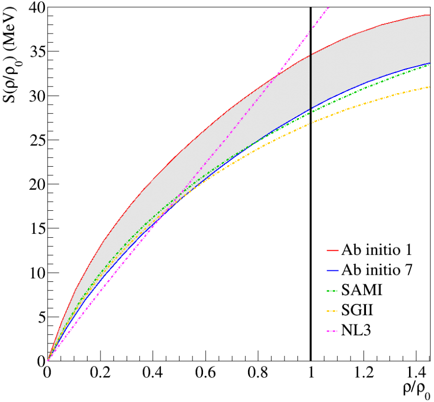

Constraint on the nuclear EoS

Procedure for experimental-simulated data comparison

At each value of ρ/ρ_0:

- Pick $S(\rho/\rho_0)$ values for the 5 nEoS parametrizations

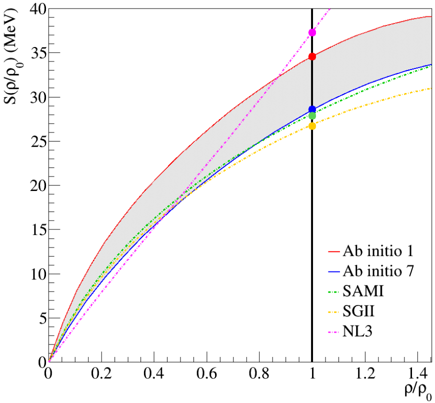

Constraint on the nuclear EoS

Procedure for experimental-simulated data comparison

At each value of ρ/ρ_0:

- Pick $S(\rho/\rho_0)$ values for the 5 nEoS parametrizations
- Plot the 5 χ^2 values as a function of the $S(\rho/\rho_0)$ for the corresponding nEoS

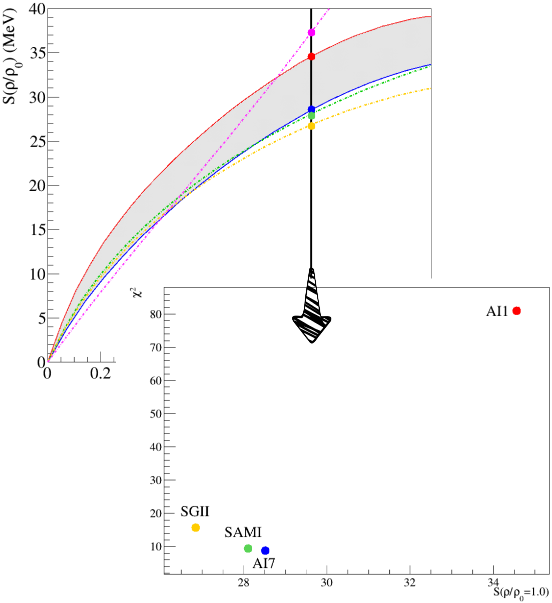

Constraint on the nuclear EoS

Procedure for experimental-simulated data comparison

At each value of ρ/ρ_0:

- Pick $S(\rho/\rho_0)$ values for the 5 nEoS parametrizations
- Plot the 5 χ^2 values as a function of the $S(\rho/\rho_0)$ for the corresponding nEoS
- Quadratic fit $\rightarrow$ parabolic dependence $\chi^2(S(\rho/\rho_0))$ around its minimum

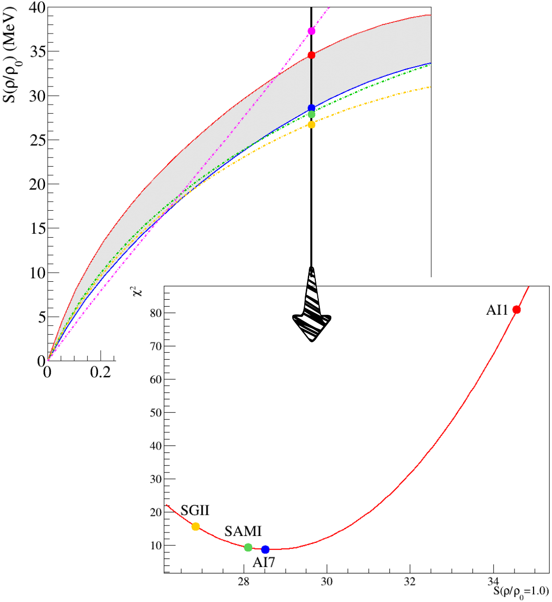

Constraint on the nuclear EoS

Procedure for experimental-simulated data comparison

At each value of ρ/ρ_0:

- Pick $S(\rho/\rho_0)$ values for the 5 nEoS parametrizations
- Plot the 5 χ^2 values as a function of the $S(\rho/\rho_0)$ for the corresponding nEoS
- Quadratic fit → parabolic dependence $\chi^2(S(\rho/\rho_0))$ around its minimum

Repeat along the ρ/ρ_0 axis.

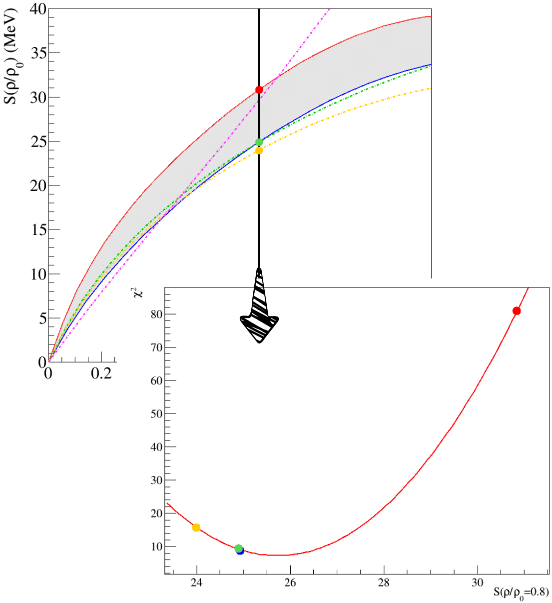

At each value of ρ/ρ_0:

- Pick $S(\rho/\rho_0)$ values for the 5 nEoS parametrizations
- Plot the 5 χ^2 values as a function of the $S(\rho/\rho_0)$ for the corresponding nEoS
- Quadratic fit $\rightarrow$ parabolic dependence $\chi^2(S(\rho/\rho_0))$ around its minimum

Repeat along the ρ/ρ_0 axis.
At each ρ/ρ_0 we thus define a likelihood along $S(\rho/\rho_0)$ as:

$$\mathcal{L}(S(\rho/\rho_0)) \propto e^{-\chi^2(S(\rho/\rho_0))/2}$$

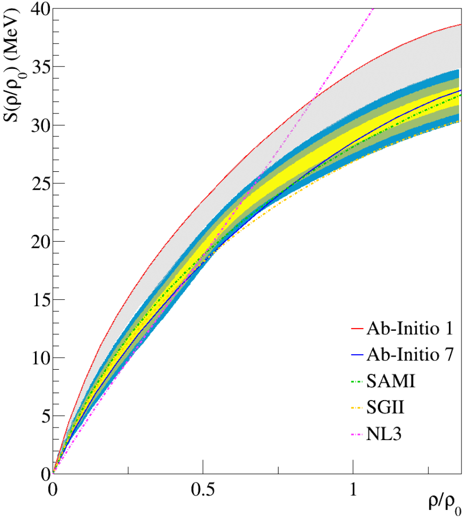

At each value of ρ/ρ_0:

- Pick $S(\rho/\rho_0)$ values for the 5 nEoS parametrizations
- Plot the 5 χ^2 values as a function of the $S(\rho/\rho_0)$ for the corresponding nEoS
- Quadratic fit $\rightarrow$ parabolic dependence $\chi^2(S(\rho/\rho_0))$ around its minimum

Repeat along the ρ/ρ_0 axis.
At each ρ/ρ_0 we thus define a likelihood along $S(\rho/\rho_0)$ as:

$$\mathcal{L}(S(\rho/\rho_0)) \propto e^{-\chi^2(S(\rho/\rho_0))/2}$$

Consider the density region probed with isospin diffusion $\rightarrow$ *weight function*

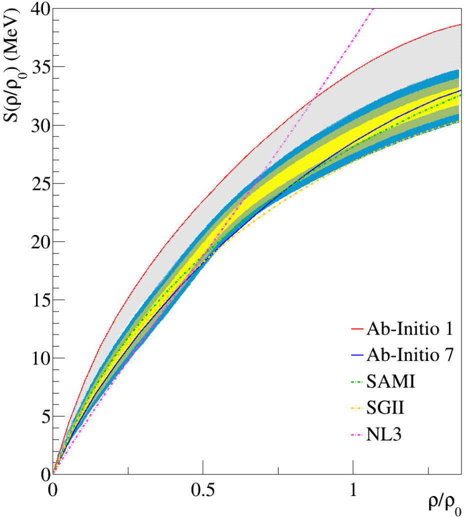

Constraint on the nuclear EoS
Bayesian framework

The proposed procedure corresponds to a **Bayesian parameter estimation**

- of the value of the symmetry energy at different densities $S_i = S(\rho_i)$
- **not** of the nuclear matter parameters $S_i \propto \frac{d^i E_{sym}}{d\rho^i}(\rho_0)$ (derivatives at saturation)

The posterior marginalized distribution of S_i is given by:

$$p(S_i) = \frac{1}{N}\sum_{m=1}^{N} p(m|\vec{d})\,\delta\left(S_i - S_i^{(m)}\right) \qquad \text{where} \qquad p(m|\vec{d}) = \mathcal{N} p^{prior}(m) p(\vec{d}|m)$$

- the set of data $\vec{d} = \{d_1, \ldots, d_K\}$ is the set of ITR data points $d_j = R(b_j)$
- we consider a gaussian likelihood $p(\vec{d}|m) \equiv \mathcal{L}_{\vec{d}}(m) = \exp\left(-\chi^2_m/2\right)$ with $\chi^2_m = \sum_{j=1}^{K}(d_j - d_j^{(m)})^2/\sigma^2_{jm}$ and $\sigma^2_{jm} = \sigma^2_{exp,j} + \sigma^2_{th,jm}$
- we take a flat constant prior $p^{prior}(S(\rho_i))$ for each density ρ_i, to which we apply the weight function $p_i^{prior} = w(\rho_i/\rho_0)$, as a confidence factor on the density axis.
  $\Rightarrow$ globally $p_i(m|ITR) = w(\rho_i/\rho_0)\exp\left(-\chi^2_m/2\right)$

Constraint on the nuclear EoS

Sensitive density region: radius of the examination sphere

The values of baryonic density and isospin current density depend on the radius of the spherical volume used for their evaluation.

- For $r > 3$ fm the sphere extends beyond the neck region (including empty areas), which reduces both the density and the current density
- For $r < 3$ fm, the finite number of test particles within the sphere introduces strong statistical fluctuations that affect the current evaluation

The radius equal to 3 fm has been chosen as the optimal value, balancing these competing effects.

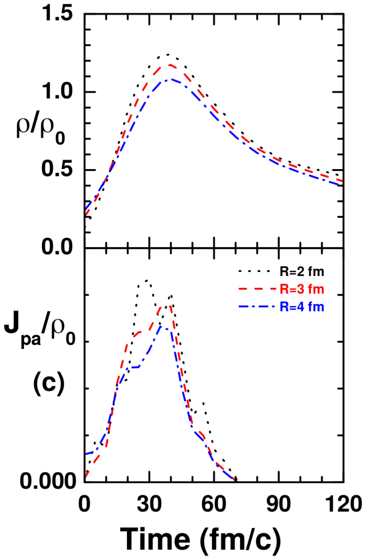

The confidence regions slightly depend on the choice of b and t intervals for the weight function, but our observations are stable against these arbitrary choices.

0fm/c–80fm/c

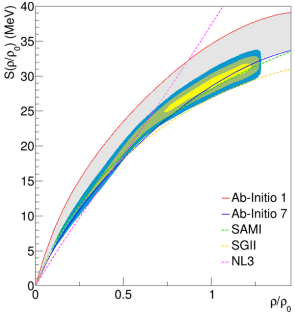

15fm/c–80fm/c

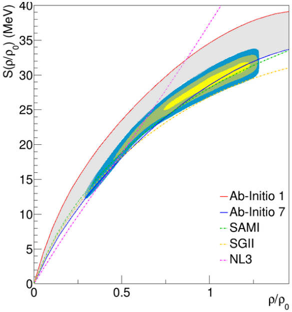

0fm/c–60fm/c

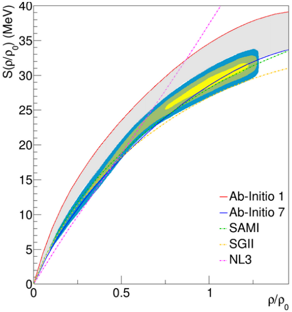

e.g., varying the time interval for the weight function evaluation essentially changes the contribution from the low density tail.